Channel Dynamics in Mobile-to-Mobile Communications: Recent Results and Challenges

Claude Oestges*, Gloria Makhoul†, Raffaele D'Errico†, Evgenii Vinogradov‡
*ICTEAM Electrical Engineering, Université catholique de Louvain (UCLouvain), Louvain-la-Neuve, Belgium
†CEA-LETI, Grenoble, France
‡ KU Leuven, Department of Electrical Engineering - ESAT, Leuven Belgium
Email: claude.oestges@uclouvain.be, {gloria.makhoul, raffaele.derrico}@cea.fr, evgenii.vinogradov@esat.kuleuven.be

***Abstract*—Recent results about mobile-to-mobile radio channel dynamics are analyzed, considering indoor peer-to-peer, body-centric and vehicule-to-pedestrian transmissions. Investigations are based on various experimental campaigns from 2.4 to 4 GHz. Regarding peer-to-peer and body-centric scenarios, measurements conducted in room-to-room and in-room environments show a strong non-stationary behavior, modeled by a Markov chain-based approach. In the vehicular context, several vehicular-to-pedestrian scenarios with different mobility patterns are investigated and channel statistics are derived.**

I. Introduction

MOBILE-TO-MOBILE (M2M) communication networks have emerged as a powerful solution to enhance the quality of data service with low energy consumption. Examples of M2M networks include e.g. mobile peer-to-peer, body-centric and vehicle-to-pedestrian (V2P) applications. However, the inherent dual mobility generates non-stationarity properties of the propagation channel, implying that accurate dynamic models are required for system design and network simulation.

On the one hand, peer-to-peer and wireless body area networks (WBANs) typically consist of transceiver nodes placed on or in the vicinity of the human body and encompass a large number of applications, such as cooperative communications, e-health, remote monitoring, sports and entertainment [1]. Understanding the radio channel behavior is critical to develop efficient body-centric communications systems, especially when relay and cooperative techniques are considered to overcome the severity of on-body path-loss and/or body shadowing [2]. In particular, the prediction and modeling of channel dynamics may strongly differ from classical wireless transmissions, especially in the case of body-to-body (B2B) transmissions [3], [4].

On the other hand, vehicle-to-X (V2X) communications have received a significant attention in the recent years for road safety based on intelligent transportation systems (ITS). As a result, the IEEE 802.11p standard was developed for dedicated short range communication (DSRC) [5]. For vehicle-to-vehicle (V2V) channels, the channel non-stationarity stems from the dynamic change of the environments around both mobile terminals. The two major approaches that can include this aspect are the tapped delay line (TDL) model including birth/death process to account the appearance and disappearance of taps [6], [7] and the geometry-based stochastic channel modeling (GSCM) [8], [9]. The V2P channels are defined as a direct link between moving vehicles and a wide set of road passengers, e.g. pedestrians, bicyclists etc. So far, only [10], [11] have investigated V2P channel statistics based on experimental data.

In this communication, we summarize recent results focusing on the characterization and modeling of M2M channel dynamics, including non-stationary behaviors. To this end, we rely on recent results on indoor peer-to-peer, body-centric and vehicle-to-pedestrian transmissions.

II. Peer-to-Peer Indoor Transmissions

In [12], a peer-to-peer measurement campaign was carried out in two environments: subjects were either grouped in a large room or isolated in different rooms (the latter being represented in Figure 1, upper graph). In both cases, they moved freely on their own, avoiding regular motions. The experimental set-up relied on the use of UCL Elektrobit Propsound MIMO channel sounder, used in a distributed fashion [13] at the frequency of 3.8 GHz. The distributed body nodes were connected to the sounder by multiple 32-meter low-loss RF cables.

Based on this experimental campaign, small-scale fading was found to strongly differ from one stationarity period to the next one, and its distribution ranged from double-Rayleigh to highly Ricean. In [12]–[14], we showed that this type of fading could be described by a single distribution, consisting of a weighted combination of line-of-sight (with weight ω_0), Rayleigh (with weight ω_1) and Double-Rayleigh (with weight ω_2) contributions, whose probability density function is given by:

$$\rho_{SOSF}(g) = \int_0^\infty \omega e^{-\omega_1^2\omega^2/4} \frac{4J_0(g\omega)J_0(\omega_0\omega)}{4+\omega_2^2\omega^2} \, d\omega \quad (1)$$

where g is the fading amplitude, J_0 is the Bessel function of the first kind and zeroth order. Normalizing $\mathbb{E}\{g^2\} = 1$, we have that $\omega_0^2 + \omega_1^2 + \omega_2^2 = 1$ and we can parametrize the distribution by two factors [14]

$$\alpha = \frac{\omega_2^2}{\omega_0^2+\omega_1^2+\omega_2^2} \qquad \beta = \frac{\omega_0^2}{\omega_0^2+\omega_1^2+\omega_2^2} \quad (2)$$

where (α, β) are constrained to the triangle $\alpha \geq 0$, $\beta \geq 0$, and $\alpha + \beta \leq 1$.

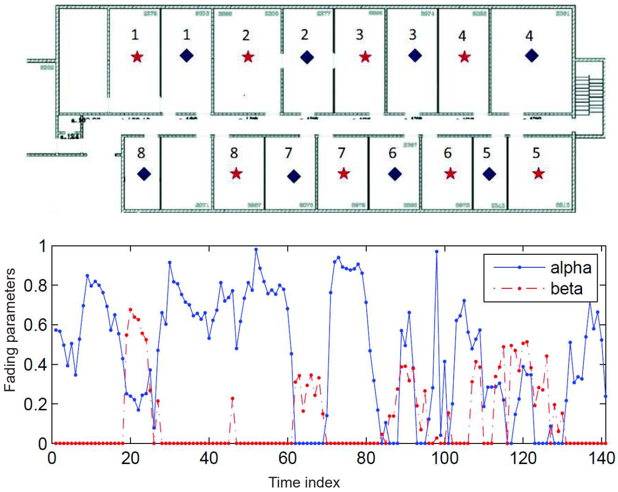

Fig. 1. Upper: Body-to-body configuration (stars are receive nodes, diamonds are transmit nodes); lower: Variation of fading parameters along time (total duration is 113 s)

The lower graph of Figure 1 illustrates the variation of the characteristic fading parameters (α and β) as time evolves. The horizontal axis represents time index at the rate of 1.25 Hz. Interestingly, α varies significantly from Rayleigh ($\alpha \approx 0$) to double-Rayleigh ($\alpha \rightarrow 1$), whereas the channel sometimes contains a fixed component ($\beta > 0$). Double-Rayleigh fading is actually observed when wave-guiding takes place along the corridor, which tunnels the energy from one room to another room (this mechanism was not measured when rooms were separated by plasterboard partitions). To model the transitions between fading states, a hidden-Markov model [12] can be used.

III. Body-to-Body Networks

Body-to-body communications consist in transmissions between different bodies, or more generally, persons, who can be located in the same room or in neighboring rooms. Several authors have recently investigated such channels, which can be characterized by a highly non-stationary behavior [3], [4], [15], [16]. Most studies usually assume that the channel is stationary: while this is justified in specific experimental scenarios, it is likely that typical body motion and shadowing will induce non-stationary conditions. In [17], the time correlation functions of B2B fading channels for different mobility patterns is analytically modeled based on a measurement campaign carried out in an indoor environment at 2.48 GHz. A general framework for the time correlation function modeling is developed assuming a typical M2M propagation scenario where some human subjects are moving in a room at the same velocity v (along the same or the opposite direction) whereas local scatterers are moving with random velocities and in random directions. To validate the model, the experimental scenarios depicted in Figure 2 are as follows: transmitter A and receiver B are moving simultaneously in the same direction whereas two scatterers (i.e. two other subjects, C and D) are walking in the opposite direction (scenario 1); transmitter A and receiver C are moving simultaneously in opposite directions whereas two scatterers (i.e. two other subjects, B and D) are also walking in opposite directions (scenario 2). Applying a general framework to these cases, the time correlation $R(\Delta t)$ can be represented for parallel walks by

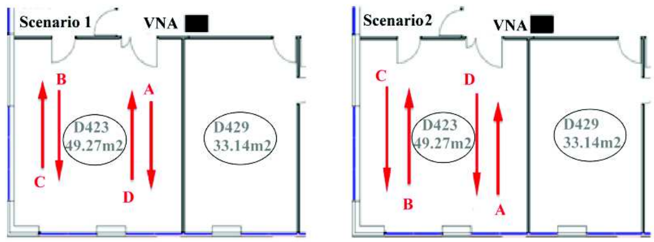

(a) Scenario 1 (b) Scenario 2

Fig. 2. Experimental B2B propagation scenarios with two terminals and two (human) moving scatterers

$$
\begin{aligned}
&R(\Delta t) = \\
&a\sum_{n,m=-\infty}^{+\infty}(-1)^{(n+m)}\gamma_{nm}J_n(4\pi\nu_D\Delta t)J_m(4\pi\nu_D\Delta t) \\
&+(1-a)\sum_{n,m=-\infty}^{+\infty}(-1)^{n+m}\gamma_{nm}J_n(2\pi\nu_D\Delta t)J_m(2\pi\nu_D\Delta t)
\end{aligned} \tag{3}
$$

where $\nu_D = v/\lambda$ is the maximum Doppler frequency shift due to the mobility of the terminals, γ_{nm} are the coefficients of the double Fourier series of the joint azimuth power spectrum for a random point in the room and a is the share of scatterers moving at the same speed, in parallel to the terminals (e.g. other persons in the room). For two human subjects walking in opposite directions, $R(\Delta t)$ becomes

$$
\begin{aligned}
R(\Delta t) &= \sum_{p=-\infty}^{+\infty}(b\gamma_{0p} + (-1)^p d\gamma_{p0})J_p(4\pi\nu_D\Delta t) \\
&+(1-b-d)\sum_{n,m=-\infty}^{+\infty}(-1)^n\gamma_{nm}J_n(2\pi\nu_D\Delta t)J_m(2\pi\nu_D\Delta t)
\end{aligned} \tag{4}
$$

where b and d represent the share of scatterers moving in opposite directions (i.e. subjects B and D in scenario 2).

Figure 3 illustrates a comparison between the measured correlation function for both scenarios and equations (3) and (4), applied with $a = 2b = 2d = 0.09$ and where the γ_{nm} coefficients are estimated up to the first or tenth order (the isotropic case is obtained when γ_{nm} is non-zero and equal to 1 only for $n = m = 0$). The impact of the two moving scattering humans is clearly significant.

IV. Vehicle-to-Pedestrian Communications

A V2P channel measurement campaign was carried out using UCLouvain channel sounder at 3.8 GHz with a measurement bandwidth B of 200 MHz [18]. Dipole antennas

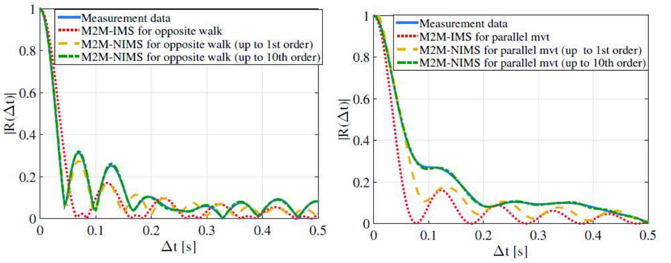

Fig. 3. Experimental B2B results for both scenarios, with moving scatterers isotropically distributed (IMS) or distributed along lines (NIMS, with various orders in the summation)

were used at both transmit (Tx) and receive (Rx) terminals, the Tx antenna being mounted on a car roof with the Rx antenna carried by a pedestrian. The experimental environments include a two-lane avenue, as well as a courtyard entrance, with the pedestrian on the sidewalk or entering the yard. The vehicle speed was around 30 km/h and the V2P distance varied from of 2 m to 40 m depending on the scenario. The time varying channel impulse response can be divided into three major components: the strongest path which mainly consists of the line-of-sight and ground reflection paths; the discrete components arising from specular reflection of scatterers; the diffuse components resulting from multiple-scattering diffraction that cannot be associated with the discrete components. Regarding the strongest path and the discrete components [18],

- the path loss is modeled by a two-ray approach for the former, while the latter is characterized by a classical path-loss exponent, whose value varies from 1.3 to 5.2 depending on the scenario;
- the large-scale fading is modeled as a lognormal variable (with a standard deviation varying between 1.8 and 4.9 dB), and its dynamics follow an exponential auto-correlation function in time (with a coherence time around 0.5 s for the strongest path and around 1.5 s for the discrete multipaths);
- the small-scale fading is Ricean for the first path and close to Rayleigh for the remaining paths.

V. Conclusions

In this paper, we have illustrated through various measurement-based models that peer-to-peer, body-centric and vehicle-to-pedestrian communications, being doubly-mobile, are often far from stationary. This non-stationarity has a significant impact on the channel models and signal processing techniques to be developed, as real-world propagation may strongly deviate from the behavior obtained in canonical scenarios.

VI. Acknowledgments

This research was carried out within EU-COST IC1004 and CA15104 (IRACON) Actions. The authors are pleased to acknowledge the collaboration of Dr. P. Pasquero and Dr. F. Mani (CEA-LETI, France) as well as Dr. Nicolai Czink (previously with FTW, Austria).

References

[1] H. Cao, V. Leung, C. Chow, and H. Chan, “Enabling technologies for wireless body area networks: A survey and outlook,” *Communications Magazine, IEEE*, vol. 47, no. 12, pp. 84 –93, dec. 2009.

[2] P. Ferrand, J.-M. Gorce, and C. Goursaud, “On the packet error rate of correlated shadowing links in body-area networks,” in *Proceedings of the 5th European Conference on Antennas and Propagation (EUCAP),*, 2011, pp. 3094–3098.

[3] R. Rosini, R. Verdone, and R. D’Errico, “Body-to-body indoor channel modeling at 2.45 GHz,” *IEEE Transactions on Antennas and Propagation*, vol. 62, no. 11, pp. 5807–5819, 2014.

[4] S. L. Cotton and W. G. Scanlon, “The kappa-mu distribution applied to the analysis of fading in body to body communication channels for fire and rescue personnel,” *IEEE Antennas and Wireless Propagation Letters*, vol. 7, pp. 66–69, 2008.

[5] “Draft amendment to wireless LAN medium access control (MAC) and physical layer (PHY) specifications: Wireless access in vehicular environments,” *IEEE P802.11p/D0.26*, pp. 1–52, Jan 2006.

[6] I. Sen and D. W. Matolak, “Vehicle–vehicle channel models for the 5-GHz band,” *IEEE Transactions on Intelligent Transportation Systems*, vol. 9, no. 2, pp. 235–245, 2008.

[7] R. He, O. Renaudin, V.-M. Kolmonen, K. Haneda, Z. Zhong, B. Ai, and C. Oestges, “A dynamic wideband directional channel model for vehicle-to-vehicle communications,” *IEEE Transactions on Industrial Electronics*, vol. 62, no. 12, pp. 7870–7882, 2015.

[8] J. Karedal, F. Tufvesson, N. Czink, A. Paier, C. Dumard, T. Zemen, C. F. Mecklenbrauker, and A. F. Molisch, “A geometry-based stochastic mimo model for vehicle-to-vehicle communications,” *IEEE Transactions on Wireless Communications*, vol. 8, no. 7, pp. 3646–3657, 2009.

[9] O. Renaudin, V. M. Kolmonen, P. Vainikainen, and C. Oestges, “Wideband measurement-based modeling of inter-vehicle channels in the 5-GHz band,” *IEEE Transactions on Vehicular Technology*, vol. 62, no. 8, pp. 3531–3540, Oct 2013.

[10] Y. Ibdah and Y. Ding, “Mobile-to-mobile channel measurements at 1.85 GHz in suburban environments,” *IEEE Transactions on Communications*, vol. 63, no. 2, pp. 466–475, Feb 2015.

[11] M. G. Doone, S. L. Cotton, and C. Oestges, “An experimental investigation into the impact of vehicular traffic on interpersonal wearable-to-wearable communications channels,” *IEEE Transactions on Antennas and Propagation*, vol. 65, no. 10, pp. 5418–5430, September 2017.

[12] E. Vinogradov, W. Joseph, and C. Oestges, “Measurement-based modeling of time-variant fading statistics in indoor peer-to-peer scenarios,” *Antennas and Propagation, IEEE Transactions on*, vol. 63, no. 5, pp. 2252–2263, May 2015.

[13] C. Oestges, N. Czink, B. Bandemer, P. Castiglione, F. Kaltenberger, and A. Paulraj, “Experimental characterization and modeling of outdoor-to-indoor and indoor-to-indoor distributed channels,” *IEEE Transactions on Vehicular Technology*, vol. 59, no. 5, pp. 2253–2265, Jun 2010.

[14] B. Bandemer, C. Oestges, N. Czink, and A. Paulraj, “Physically motivated fast-fading model for indoor peer-to-peer channels,” *Electronics Letters*, vol. 45, no. 10, pp. 515–517, May 2009.

[15] S. Cotton, G. Conway, and W. Scanlon, “A time-domain approach to the analysis and modeling of on-body propagation characteristics using synchronized measurements at 2.45 GHz,” *Antennas and Propagation, IEEE Transactions on*, vol. 57, no. 4, pp. 943 –955, april 2009.

[16] Y. Wang, I. B. Bonev, J. O. Nielsen, I. Z. Kovacs, and G. F. Pedersen, “Characterization of the indoor multiantenna body-to-body radio channel,” *IEEE Transactions on Antennas and Propagation*, vol. 57, no. 4, pp. 972–979, 2009.

[17] G. Makhoul, F. Mani, R. D’Errico, and C. Oestges, “On the modeling of time correlation functions for mobile-to-mobile fading channels in indoor environments,” *IEEE Antennas and Wireless Propagation Letters*, vol. 16, pp. 549 – 552, 2017.

[18] G. Makhoul, R. D’Errico, and C. Oestges, “Wideband vehicle to pedestrian propagation channel characterization and modeling,” in *2018 12th European Conference on Antennas and Propagation (EUCAP),*, April 2018.